ACTA CHEMICA SCANDINAVICA 17 (1963) 657–666

Galvanostatic Studies of the Hydrogen Evolution Reaction on Black Nickel Electrodes

ODD RIISØEN

Chr. Michelsen Institute, Dept. of Applied Physics, Bergen, Norway

The time dependence of the hydrogen overvoltage at nickel electrodes at constant current is related to the rate of change of the degree of coverage of the electrode with atomic hydrogen during evolution. Theoretical calculations are compared with experiments made on electrodes covered with 'black' nickel, and it is shown that an electrochemical desorption reaction can explain the experimental results. The stationary state of adsorbed hydrogen at equilibrium and the rate constants for the discharge reaction and the desorption reaction are estimated from the voltage/time and the voltage/current curves.

Previous results of experimental studies on the reaction mechanism of hydrogen evolution on nickel electrodes in aqueous solutions indicate that the mechanism is that of a proton discharge followed by an atomic combination or an electrochemical desorption reaction.

Bockris and Potter [1] have given the detailed kinetics from a consideration of the stationary state of surface-adsorbed hydrogen during evolution. The diagnostic criteria applicable to the results of hydrogen overvoltage measurements are the 'exchange current density' i_0, the Tafel slope b, and the stoichiometric number ν. [1,2] The authors have applied the principles to hydrogen overvoltage measurements on smooth nickel. [3] They found $b = 0.116$ V and $\nu = 2$, and assumed that the mechanism is that of a rate determining discharge reaction followed by a recombination of adsorbed hydrogen atoms. Earlier the same conclusion was drawn by Lukovtsev, Levina, and Frumkin for nickel in HCl solutions. [4] Horiuti and Okamoto [5], however, rejected the slow discharge mechanism. They based their concepts of the mechanism of hydrogen evolution essentially on studies of the electrolytic separation factor of deuterium, and were led to the dual theory that either the catalytic or the electrochemical mechanism are in operation. A thorough discussion is given in a recently presented paper by Horiuti [6]. Ammar and Awad [7] studied the hydrogen overvoltage at electrodeposited nickel cathodes in HCl solutions and found that the Tafel line exhibited two slopes in the linear region. They attributed their results to a dual electrochemical-catalytic mechanism at low current

densities and the electrochemical mechanism at high current densities. Peers [8] examined electrodeposited nickel cathodes in H_2SO_4. The results indicated that the mechanism of H desorption is the reaction of ion + atom.

Irreproducibility of the results of hydrogen overvoltage measurements on nickel, and the slow change of overvoltage with time at any given current density have often been ascribed to the presence of impurities [9–11]. Even under highly purified conditions, however, slow time variations of overvoltage are observed. The theoretical scheme proposed by Peers [8] for the mechanism allowed for a slow change in the overvoltage with time. Previously he attributed the slow overvoltage change to a specific adsorption of anions [12,13]. Bockris and Potter assumed that the slow change in the overvoltage with time at constant current is due to the surcharging of the metal with hydrogen.

In the work presented in this paper, the time dependence of the overvoltage is studied and related to the change of the degree of coverage with time. The aim of the work is to study the hydrogen overvoltage, and to determine the mechanism of hydrogen evolution on nickel electrodes specially treated by covering the metal with a layer of nickel 'black'.

REACTION MECHANISMS

For nickel in alkaline solutions the mechanism of the hydrogen evolution is assumed to be that of a proton discharge from a water molecule followed by an atomic combination or an electrochemical desorption reaction. The reactions participating in the formation of molecular hydrogen at the electrode are then:

1. *The discharge reaction* (Me being a metal atom)

$$Me + H_2O + e^- \rightleftharpoons MeH + OH^-$$

2. *The electrochemical reaction*

$$MeH + H_2O + e^- \rightleftharpoons Me + H_2 + OH^-$$

3. *The combination reaction*

$$MeH + MeH \rightleftharpoons 2\,Me + H_2$$

For the further theoretical calculations it is assumed that the adsorbed hydrogen obeys a Langmuir isotherm, and that the only variables during the charging at constant current are the fraction of the available surface covered with atomic hydrogen, x, and the overvoltage η. The electrolyte composition, the surface properties of the electrode and the hydrogen pressure are assumed to be constant or to change very slowly in the course of time.

In the following a detailed calculation of the overvoltage/time behaviour will be presented for the case of proton discharge from water molecules followed by the electrochemical desorption reaction. It will be shown that this mechanism can explain the experimental results described later.

1. *The discharge reaction.* With the assumptions stated above, the equivalent electric currents corresponding to the reaction rates are

$$\vec{i}_1 = \vec{k}_1(1-x)\exp(-\alpha_1 zF\eta/RT) \qquad \text{(the forward current)}$$

$$\overleftarrow{i}_1 = \overleftarrow{k}_1 x \exp[(1-\alpha_1)zF\eta/RT] \qquad \text{(the reverse current)}$$

where α_1 is the fraction of the potential which affects the rate of the reaction towards the cathode. The k's are rate constants in electrical units (A cm^{-2}).

At equilibrium $\vec{i}_1 = \overleftarrow{i}_1 = i_{01}$

The net current in the forward direction is

$$i_1 = i_{01}\left\{\frac{1-x}{1-x_0}\exp\left(-\frac{\alpha_1 zF\eta}{RT}\right) - \frac{x}{x_0}\exp\left(\frac{(1-\alpha_1)zF\eta}{RT}\right)\right\} \quad (1)$$

$x = x_0$ and $\eta = 0$ are the steady state values at $i_1 = 0$.

2. *The electrochemical reaction*

$$\vec{i}_2 = \vec{k}_2 x \exp(-\alpha_2 zF\eta/RT)$$
$$\overleftarrow{i}_2 = \overleftarrow{k}_2(1-x)\exp[(1-\alpha_2)zF\eta/RT]$$

The net current is

$$i_2 = i_{02}\left\{\frac{x}{x_0}\exp\left(-\frac{\alpha_2 zF\eta}{RT}\right) - \frac{1-x}{1-x_0}\exp\left(\frac{(1-\alpha_2)zF\eta}{RT}\right)\right\} \quad (2)$$

3. *The combination reaction*

$$\vec{i}_3 = \vec{k}_3 x^2$$
$$\overleftarrow{i}_3 = \overleftarrow{k}_3(1-x)^2$$

The net current in electrical units is

$$i_3 = i_{03}\left\{\left(\frac{x}{x_0}\right)^2 - \left(\frac{1-x}{1-x_0}\right)^2\right\} \quad (3)$$

The time dependence of the overvoltage

The electric current through the electrode/electrolyte interface is given by the sum of the currents due to the discharge reaction and the electrochemical reaction

$$i = i_1 + i_2 \quad (4)$$

The rate of change of the degree of coverage x is given by the difference between the rate of adsorption and the rate of desorption

$$C_H \frac{dx}{dt} = i_1 - (i_2 + i_3) \quad (5)$$

where C_H is the adsorption capacity $= n_a \times 1.6 \times 10^{-19}$ coulomb. n_a is the number of free spaces available for adsorption of atomic hydrogen on the electrode surface. From eqns. (1)—(5) the time dependence of the overvoltage at constant current can be derived.

The initial growth of the overvoltage after a step in the external current from zero to a constant value can be assumed to be controlled by the charge of the double layer capacitor

$$i_s = i + i_c \tag{6}$$

$$i_c = -C(\mathrm{d}\eta/\mathrm{d}t) \tag{7}$$

In the following calculations the charging of the double layer capacitor is assumed to precede the charging of the electrode with hydrogen at a relatively fast rate, and $i_s = i$ for $t \geq 0$. To simplify the calculations we assume that $\alpha_1 = \alpha_2 = 0.5$, and introduce $a = xF/2RT$. If the electrochemical reaction is the desorptive reaction, eqns. (1), (2), (4), and (5) give

$$i_s = i_{01}\left(\frac{1-x}{1-x_0}\,\mathrm{e}^{-a\eta} - \frac{x}{x_0}\mathrm{e}^{+a\eta}\right) + i_{02}\left(\frac{x}{x_0}\,\mathrm{e}^{-a\eta} - \frac{1-x}{1-x_0}\,\mathrm{e}^{+a\eta}\right) \tag{8}$$

$$C_H\frac{\mathrm{d}x}{\mathrm{d}t} = i_{01}\left(\frac{1-x}{1-x_0}\,\mathrm{e}^{-a\eta} - \frac{x}{x_0}\mathrm{e}^{+a\eta}\right) - i_{02}\left(\frac{x}{x_0}\,\mathrm{e}^{-a\eta} - \frac{1-x}{1-x_0}\,\mathrm{e}^{+a\eta}\right) \tag{9}$$

At $t = 0$, $x = x_0$ and $\eta = \eta_0$
where η_0 is the initial step in the overvoltage:

$$i_s = (i_{01} + i_{02})(\mathrm{e}^{-a\eta_0} - \mathrm{e}^{+a\eta_0}) \tag{10}$$

The rate of change of the overvoltage immediately after the first voltage step can easily be calculated. At $t = 0$, where $x = x_0$, and $\eta = \eta_0$

$$\left(\frac{\mathrm{d}\eta}{\mathrm{d}t}\right)_{t=0} = -\frac{2RT}{zF}\cdot\frac{i_{01}\{x_0\mathrm{e}^{-a\eta_0} + (1-x_0)\mathrm{e}^{+a\eta_0}\} - i_{02}\{(1-x_0)\mathrm{e}^{-a\eta_0} + x_0\mathrm{e}^{+a\eta_0}\}}{\mathrm{e}^{-a\eta_0} + \mathrm{e}^{+a\eta_0}}$$

$$\cdot\frac{(i_{01}-i_{02})i_s}{(i_{01}+i_{02})^2 x_0(1-x_0)C_H} \tag{11}$$

At small current densities, where $|\eta_0| << RT/zF$

$$\left(\frac{d\eta}{dt}\right)_{t=0} = -\frac{RT}{zF}\cdot\frac{(i_{01}-i_{02})^2 i_s}{x_0(1-x_0)\,C_H(i_{01}+i_{02})^2} \tag{12}$$

For small t, the change in η with time is given by

$$\Delta\eta = \eta - \eta_0 = -\frac{RT}{zF}\cdot\frac{(i_{01}-i_{02})^2 i_s t}{x_0(1-x_0)\,C_H(i_{01}+i_{02})^2} \tag{13}$$

We assume now that either $i_{01} >> i_{02}$ or $i_{02} >> i_{01}$.
From the experimental results presented later, we find that
$x_0(1-x_0)C_H << C_H$, which gives the conditions $x_0 << 1$
or $1-x_0 << 1$. If we accept the condition $x_0 << 1$

$$\Delta\eta = -\frac{RT}{zF}\cdot\frac{i_s t}{x_0 C_H} \tag{14}$$

It is easy to see from eqn. (11), that if $i_{10} > i_{02}/x_0$ or $i_{02} > i_{01}$, $(\mathrm{d}\eta/\mathrm{d}t)$ is negative for all η_0 values, and the numerical overvoltage at constant current increases with time for all cathodic currents.

If $i_{02}/x_0 > i_{01} > i_{02}$ (15)

however, the rate of change of the overvoltage can be positive, and the numerical overvoltage decreases with time in the high c.d. range. From eqn. (11) we find that $(d\eta/dt)_{t=0}$ is positive at c.d. where

$$|\eta_0| > \frac{RT}{zF} \ln \frac{i_{01}}{i_{02}-i_{01}x_0} \tag{16}$$

and negative at c.d. where

$$|\eta_0| < \frac{RT}{zF} \ln \frac{i_{01}}{i_{02}-i_{01}x_0} \tag{17}$$

Similar calculations can be carried out in the case of a desorptive combination reaction. The equations corresponding to eqns. (8) and (9) are

$$i_s = i_{01}\left(\frac{1-x}{1-x_0}e^{-a\eta} - \frac{x}{x_0}e^{+a\eta}\right) \tag{18}$$

$$C_H\frac{dx}{dt} = i_s - i_{03}\left\{\left(\frac{x}{x_0}\right)^2 - \left(\frac{1-x}{1-x_0}\right)^2\right\} \tag{19}$$

Examination of these equations shows that a reaction path involving the combination reaction as the only desorptive reaction cannot explain the decrease in the overvoltage with time at constant current, which is experimentally observed at high current densities. At small current densities and for small t, the voltage change is given by eqn. (13).

The steady state voltage/current relation

The theory deduced above is based on the assumption of a Langmuir isotherm and it is assumed that the only variables during the charging at constant current are x and η. The simple equations are therefore only expected to be useful for the interpretation of the first part of the voltage build-up curves. We can find the values of x_0 and the rate constants $\vec{k}_1 = i_{01}$ and $\vec{k}_2 = i_{02}/x_0$ from an examination of the transient voltage build-up curves. If we substitute these values in eqns. (8) and (9) and solve them for the steady state ($dx/dt = 0$), the theoretical voltage/current curve can be plotted from

$$i_s = 2i_{01}\frac{i_{02}}{x_0}\frac{e^{-2a\eta_s} - e^{+2a\eta_s}}{\left(i_{01}+\frac{i_{02}}{x_0}\right)e^{-a\eta_s} + \frac{i_{01}}{x_0}e^{+a\eta_s}} \tag{20}$$

EXPERIMENTAL

Apparatus and procedure. The electrolytic cell built from acrylic plastic (Plexiglas) is shown in Fig. 1. The cell was designed so that the current density would be the same on each side of the cathode. The reference electrode (R) in the side compartment was made of spectrographically pure platinum covered with 'black' platinum, and the anode (A) was a bright platinum electrode. All electrodes were made of foils spotwelded to wires of the same metal. The 'black' nickel cathodes (C) were prepared after the recipe of

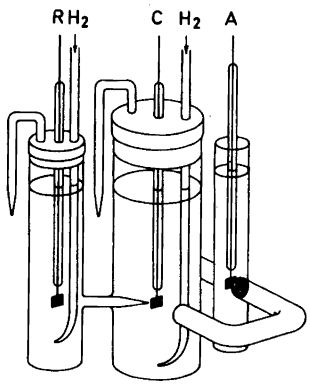

Fig. 1. The electrolytic cell.

Berezina and collaborators [14]. The deposition of nickel-black on spectrographically pure nickel sheets was effected in a solution containing 33 g/liter of nickel and ammonium double sulphate and 14 g/liter of potassium sodium tartrate at a current density of 0.1 A cm^{-2} in 2 min. The prepared electrodes were immersed in 1 N carbonate-free KOH and anodically polarized at 10^{-2}A cm^{-2} in 1 min. After activation by cathodic polarization in the electrolytic cell, the rest potentials were within 3 mV of the reversible hydrogen potential and always positive. Makrides and Coltarp [11] cleaned nickel electrodes in an analogous manner. They assumed that impurities were displaced by negative ions, and that on reducing the passive layer by cathodic polarization, clean nickel electrodes were produced. Carbonate-free KOH solution was prepared by a recipe by Powell and Hiller [15] from reagent grade KOH and $Ba(OH)_2$. Pre-electrolysis was carried out in the cell on a black nickel cathode and a platinum anode, and continued for about 20 h with a current of 10^{-1}A cm^{-2}. After replacing the electrodes used for pre-electrolysis by the electrodes used for the experimental runs, hydrogen was fed into the cell and electrolyte discharged through a tap until a convenient solution level was attained. During the experiments no hydrogen was bubbled through the electrolyte in the cathode compartment. The bubbling rate in the reference electrode vessel was 2—3 bubbles per second.

The potential of the cathode was measured with respect to the black platinum hydrogen electrode. The voltage was fed into a d.c. amplifier with an input resistance > 100 MΩ and a voltage gain of one. Build-up of voltage at constant current and decay

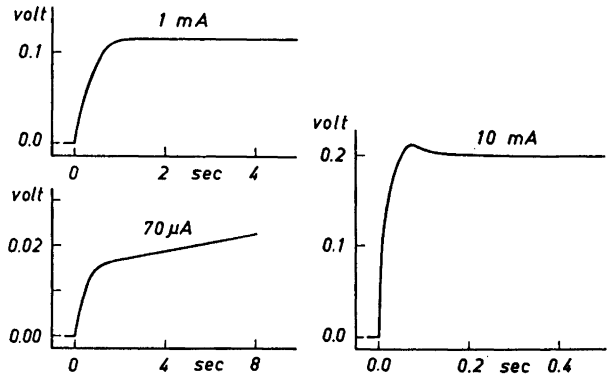

Fig. 2. Typical overvoltage build-up curves at constant current. At small c.d. the initial fast voltage growth is followed by a much slower increase, whereas at high c.d. the initial step is followed by a voltage decrease.

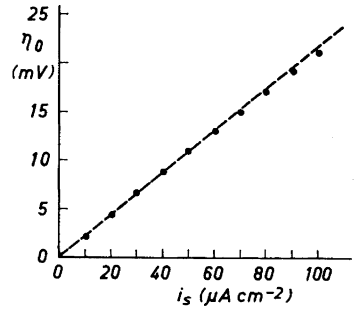

Fig. 3. The initial step in the overvoltage plotted against the current density.

on open circuit were followed on a medium speed recorder (Sefram Graphispot, Type: GR2VAD No. 488). Starting with the open circuit voltage, the growth of the voltage after switching on the current was recorded at a speed of 5 mm/sec. The current was then interrupted and the electrode potential was allowed to reach its steady state rest potential before the next run. Measurements were made in the current density range 10^{-5} to 10^{-1} A cm^{-2}. Fig. 2 shows typical overvoltage build-up curves. At small current densities the initial fast voltage growth is followed by a much slower increase which lasts for several minutes before a final steady state value is attained. At high c.d. the initial step is followed by a voltage decrease.

The resistance overvoltage was measured by superposing small square wave current pulses on the constant current, and the resistance was estimated from the initial momentary voltage step.

RESULTS AND CALCULATIONS

The experiments were carried out on a group of seven electrodes prepared in the same way. The cell was maintained at a temperature of 20°C $\pm$ 0.1° throughout the experiments.

The exchange current densities i_{01} and i_{02}. Eqn. (10) gives the relation between the initial step in the overvoltage, η_0, and the constant current i_s. For $|\eta_0| < RT/zF$ eqn. (10) reduces to

$$i_s = -(i_{01} + i_{02})\,(RT/zF)\,\eta_0$$

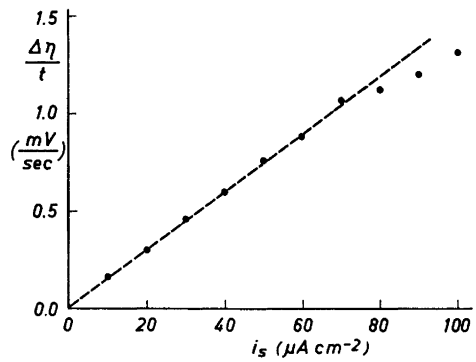

Fig. 4. The rate of change of the overvoltage after the initial voltage step, plotted against the current density.

Table 1.

Electrode No.	$i_{01} + i_{02}$ A cm^{-2}	$x_0 C_H$ coulomb	C μF	f	x_0
1	1.10×10^{-3}	1.6×10^{-3}	2100	130	0.077
2	0.13	1.7	2700	165	0.064
3	0.11	1.6	2300	140	0.071
4	0.12	1.7	2600	160	0.066
5	0.13	1.75	2800	175	0.062
6	0.12	1.45	2500	155	0.059
7	0.12	1.5	2500	155	0.060

Fig. 3 shows the experimental values of η_s plotted against i_s at small current densities. The points lie on a straight line in accordance with theory. From the slope of this line ($i_{01} + i_{02}$) was found.

The number of sites occupied by atomic hydrogen. After the initial voltage step, the overvoltage seemed to increase linearly with time for the first few seconds at small current densities, and the change in the overvoltage, $\Delta\eta$, could be described by eqn. (14). In Fig. 4 $\Delta\eta/t$ is plotted against i_s. The number of sites occupied by atomic hydrogen at equilibrium, $n_H = x_0 C_H/e_0$, was found from the slope of the experimentally obtained straight line. $e_0 = 1.6 \times 10^{-19}$ coulomb is the charge on a hydrogen ion.

Calculation of x_0. The 'roughness' factor (f) of the electrode was calculated from the differential capacity (C) of the electrode. The capacity could be derived from the time constant of the initial voltage build-up curve. For $|\eta| << RT/zF$ we find from eqns. (6), (7), and (10)

$$\eta = \eta_0(1-e^{-t/\tau}), \text{ where } \tau = \frac{RT}{zF} \cdot \frac{C}{i_{01} + i_{02}}$$

If the capacity for an 'ideal' smooth electrode has the value C_0, the 'roughness' factor is given by

$$f = C/C_0$$

If there are 10^{16} active sites per cm^2 on the smooth electrode [1], the number of active sites on the electrode under examination is

$$n_A = 10^{15} f$$

x_0 is given by

$$x_0 = n_H/n_A$$

The calculations are carried out for $C_0 = 16\ \mu F$ [16].

The experimental values of ($i_{01} + i_{02}$), $x_0 C_H$ and C are tabulated in Table 1 together with the calculated values of f and x_0.

Steady state overvoltage/current curves

Fig. 5 shows experimentally obtained steady state overvoltage values plotted against $\log_{10}$ current density. The full line represents the theoretical polarization curve, calculated from eqn. (20) with $i_{02} = 10\ \mu$A cm^{-2}, $i_{01} = 90\ \mu$A cm^{-2}, and $x_0 = 0.09$ *.

* This value of x_0 is different from the value tabulated in Table 1. The calculation of the latter is, however, based on a rough estimation of the number of active points for a 'smooth' electrode, and cannot be expected to give an accurate value of x_0.

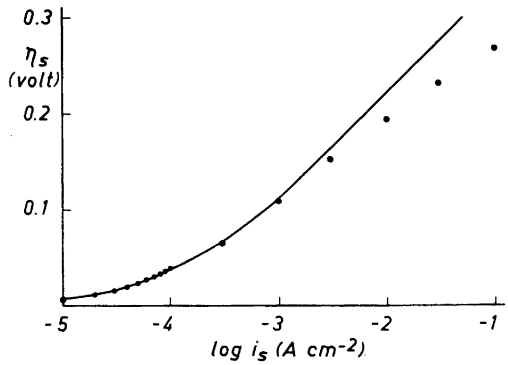

Fig. 5. Variation of the steady state overvoltage with $\log_{10}$ current density. The points are experimental values, whereas the full line is the theoretically calculated polarization curve.

Up to about 10^{-3} A cm^{-2} the experimental points lie on the theoretical curve, but at greater current densities the theory, as expected, does not explain the experimental results. The results were reproducible, the differences between the electrodes seemed mainly to be due to the different 'roughness' factors of the electrode surfaces. Fig. 6 shows the limits for the Tafel lines. All Tafel lines lie within the shaded area.

CONCLUSIONS

The theoretical equations used to describe the experimental results are based on a simple reaction scheme, involving a proton discharge from a water molecule followed by an electrochemical desorption reaction. The time dependence of the overvoltage at constant current is related to the rate of change of the degree of coverage of the electrode with atomic hydrogen. It is assumed that η, x, and i are the only variable quantities, and that the adsorbed hydrogen obeys a Langmuir isotherm. Within the limits given by the idealized assumptions the experimental results are in good accordance with the theory.

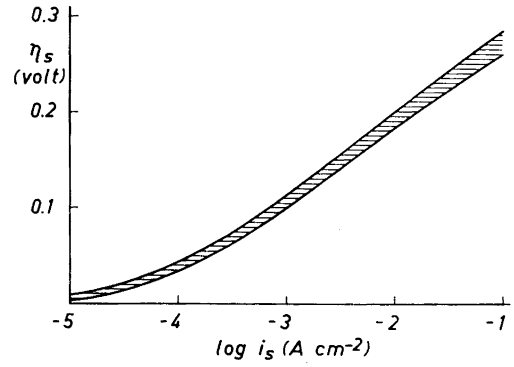

Fig. 6. The limits for the Tafel lines for the group of examinated electrodes.

The time constants for the overvoltage transients after a change in the current could be found from the theoretical equations to be several minutes at small current densities, and the 'rapid' method of establishing the Tafel lines, used by Bockris and Potter [3], does not give steady state conditions.

The stoichiometric number, ν, and the Tafel slope, b, found from the polarization curves are commonly used to differentiate between the three main reactions of the hydrogen evolution. If there is a rate-determining reaction, ν will be either 1 or 2.

It is, however, easy to find from eqn. (20) and the experimental results that both the discharge and the electrochemical reaction determine the rate of the whole reaction. The shape of the polarization curve is therefore not described by well-defined characteristic values of ν and b.

The rapid method, and the use of the stoichiometric number as a diagnostic criterium seem, however, to be useful to establish the reaction scheme for the 'smooth' nickel electrodes examined by Bockris [3]. The reaction path is proposed to be the slow discharge followed by an atomic combination reaction. With the same assumptions as used in this paper it can be shown that this reaction scheme will give the characteristic value $\nu = 2$, and that the rapid method can be used to establish the Tafel lines. If the reaction path and the rate constants are the same for 'smooth' and 'black' nickel cathodes, the Tafel lines will be similar if one reduces the current density by the 'roughness' factor. This is, however, not the case, the Tafel lines presented in this paper for 'black' nickel cathodes do not coincide with those found on smooth nickel cathodes [3,16], but have the same shape as the Tafel lines found by Peers [8] on his group I of electrodeposited nickel cathodes. It is therefore reasonable to suppose that 'smooth' and 'black' electrodes are not subject to the same reaction mechanism, and that comparisons of experimental results only can be made for electrodes prepared in the same way.

Acknowledgement. This work was supported by the *Royal Norwegian Council for Scientific and Industrial Research.*

REFERENCES

1. Bockris, J. O'M. and Potter, E. C. *J. Electrochem. Soc.* **99** (1952) 169.
2. Bockris, J. O'M. and Conway, B. E. *Modern Aspects of Electrochemistry*, Butterworths Scientific Publications 1954, Chapter 4.
3. Bockris, J. O'M. and Potter, E. C. *J. Chem. Phys.* **20** (1952) 614.
4. Lukovtsev, P., Levina, S. and Frumkin, A. *Acta Physicochim. URSS* **11** (1939) 21—44.
5. Horiuti, J. and Okamoto, G. *Sci. Papers Inst. Phys. Chem. Res. (Tokyo)* **28** (1936) 231.
6. Horiuti, J. *Transactions of the Symposium on Electrode Processes*, The Electrochem. Soc. Series, John Wiley & Sons, New York, London 1959, Paper 2.
7. Ammar, I. A. and Awad, S. A. *J. Phys. Chem.* **60** (1956) 837.
8. Peers, A. M. *J. Chim. Phys.* **58** (1960) 338.
9. Bockris, J. O'M. and Conway, B. E. *Trans. Faraday Soc.* **45** (1949) 989.
10. Azzam, A. M., Bockris, J. O'M. and Rosenberg, H. *Trans. Faraday Soc.* **46** (1950) 918.
11. Makrides, A. C. and Coltharp, M. T. *J. Electrochem. Soc.* **107** (1960) 472.
12. Peers, A. M. *J. Chim. Phys.* **57** (1960) 356.
13. Kolotyrkin, Ya. M. *Trans. Faraday Soc.* **55** (1959) 455.
14. Berezina, S. N., Vozdvizhensky, G. S. and Deziderye v, G. P. *J. Appl. Chem. USSR* **25** (1952) 1057.
15. Powell, J. E. and Hiller, M. A. *J. Chem. Educ.* **34** (1957) 330.
16. Devanathan, M. A. and Selvaratnam, M. *Trans. Faraday Soc.* **58** (1960) 1820.

Received September 10, 1962.